



HAL
open science

Degradation and deactivation of a plasmid-encoded extracellular antibiotic resistance gene during separate and combined exposures to UV254 and radicals

Maolida Nihemaiti, Younggun Yoon, Huan He, Michael C. Dodd,
Jean-Philippe Croué, Yunho Lee

► To cite this version:

Maolida Nihemaiti, Younggun Yoon, Huan He, Michael C. Dodd, Jean-Philippe Croué, et al.. Degradation and deactivation of a plasmid-encoded extracellular antibiotic resistance gene during separate and combined exposures to UV254 and radicals. *Water Research*, 2020, 182, pp.115921 -. 10.1016/j.watres.2020.115921 . hal-03492495

HAL Id: hal-03492495

<https://hal.science/hal-03492495>

Submitted on 15 Jul 2022

HAL is a multi-disciplinary open access archive for the deposit and dissemination of scientific research documents, whether they are published or not. The documents may come from teaching and research institutions in France or abroad, or from public or private research centers.

L'archive ouverte pluridisciplinaire **HAL**, est destinée au dépôt et à la diffusion de documents scientifiques de niveau recherche, publiés ou non, émanant des établissements d'enseignement et de recherche français ou étrangers, des laboratoires publics ou privés.



Distributed under a Creative Commons Attribution - NonCommercial 4.0 International License

1 **Degradation and deactivation of a plasmid-encoded extracellular**
2 **antibiotic resistance gene during separate and combined exposures**
3 **to UV₂₅₄ and radicals**

4 Maolida Nihemaiti ^{a,1}, Younggun Yoon ^{b,1}, Huan He ^c, Michael C. Dodd ^c, Jean-Philippe Croué
5 ^{a, d, *}, and Yunho Lee ^{b, *}

6 ^a Curtin Water Quality Research Centre, Department of Chemistry, Curtin University, GPO Box
7 U1987, Perth 6845, Australia

8 ^b School of Earth Sciences and Environmental Engineering, Gwangju Institute of Science and
9 Technology (GIST), Gwangju 61005, Republic of Korea

10 ^c Department of Civil and Environmental Engineering, University of Washington, Seattle,
11 Washington 98195-2700, United States

12 ^d Institut de Chimie des Milieux et des Matériaux IC2MP UMR 7285 CNRS, Université de
13 Poitiers, France

14 ¹ M. Nihemaiti and Y. Yoon contributed equally to this work

15 *Corresponding authors: Yunho Lee, Email: yhlee42@gist.ac.kr

16 Jean-Philippe Croué, Email: jean.philippe.croue@univ-poitiers.fr

17 **Submitted to Water Research**

18 Abstract

19 This study investigated the degradation and deactivation of an extracellular ampicillin resistance
20 gene (amp^R) encoded in plasmid pUC19 during exposure to UV₂₅₄, •OH (generated by
21 UV_{>290}/H₂O₂), and combined exposure to UV₂₅₄ and •OH (SO₄^{•-}) using UV₂₅₄/H₂O₂ and
22 UV₂₅₄/S₂O₈²⁻. The degradation rates of amp^R measured by quantitative polymerase chain
23 reaction increased with increasing target amplicon length (192–851 bps). The rate constants for
24 the degradation of pUC19 (2686 bps) were calculated as 0.26 cm²/mJ for UV₂₅₄ and 1.5×10¹¹ M⁻¹
25 s⁻¹ for •OH, based on the degradation rates of amp^R amplicons and assuming an equal
26 sensitivity of DNA damage across the entire plasmid. DNA repair-proficient *Escherichia coli* (*E.*
27 *coli*) AB1157 strain (wild-type) and its repair-deficient mutants including AB1886 (*uvrA*⁻),
28 AB2463 (*recA*⁻), AB2480 (*uvrA*⁻, *recA*⁻), and DH5α (*recA*⁻, *endA*⁻) were applied as recipient
29 cells in gene transformation assays. Results suggested that the elimination efficiency of
30 transforming activity during UV₂₅₄ and •OH exposure was dependent on the type of DNA repair
31 genes in recipient *E. coli* strains. Losses of transforming activity were slower than the
32 degradation of pUC19 by a factor of up to ~5 (for *E. coli* DH5α), highlighting the importance of
33 DNA repair in recipient cell. The degradation rates of amp^R amplicons were much larger (by a
34 factor of ~4) in UV₂₅₄/H₂O₂ and UV₂₅₄/S₂O₈²⁻ than UV₂₅₄ direct photolysis, indicating the
35 significant contribution of •OH and SO₄^{•-} to the gene degradation. Not only UV₂₅₄ and SO₄^{•-},
36 but also •OH contributed to the degradation of amp^R during UV₂₅₄/S₂O₈²⁻, which was attributed
37 to the conversion of SO₄^{•-} to •OH and a 10-fold larger reactivity of •OH towards amp^R as
38 compared to SO₄^{•-}. However, the enhanced gene degradation by radicals did not lead to a faster
39 elimination of gene transforming activity during UV₂₅₄/H₂O₂ and UV₂₅₄/S₂O₈²⁻, suggesting that
40 UV₂₅₄- and radical-induced DNA damage were not additive in their contributions to losses of
41 gene transforming activity. Wastewater effluent organic matter (EfOM) accelerated the
42 degradation of amp^R during UV₂₅₄ irradiation by means of reactive species production through

43 indirect photolysis reactions, whereas EfOM mainly acted as a radical scavenger during
44 UV_{254}/H_2O_2 and $UV_{254}/S_2O_8^{2-}$ treatments.

45 **Keywords**

46 Antibiotic resistant bacteria, antibiotic resistance genes, gene transformation, UV, hydroxyl
47 radical, sulfate radical

48 **Abbreviations**

49	<i>amp^R</i>	Ampicillin Resistance Gene
50	AOPs	Advanced Oxidation Processes
51	Amp	Amplicon
52	ARB	Antibiotic Resistant Bacteria
53	ARG(s)	Antibiotic Resistance Gene(s)
54	bp(s)	Nucleotide Base Pair(s)
55	DOM	Dissolved Organic Matter
56	e-ARG	Extracellular Antibiotic Resistance Genes
57	<i>E. coli</i>	<i>Escherichia coli</i>
58	EfOM	Effluent Organic Matter
59	<i>p</i> CBA	<i>para</i> -Chlorobenzoic Acid
60	qPCR	Quantitative Polymerase Chain Reaction

61 **1. Introduction**

62 Antibiotic resistance is a natural phenomenon. However, anthropogenic activities (e.g.,
63 overuse and disposal of antibiotics) are providing constant selection pressure on antibiotic
64 resistant bacteria (ARB) (Vikesland, Pruden et al. 2017). Antibiotic resistance can be developed
65 and disseminated within the bacterial population by genetic mutation, cell division, and the
66 transfer of antibiotic resistance genes (ARGs) (Davies and Davies 2010). ARGs are
67 contaminants of concern in natural and engineered aquatic systems, as ARG transfer can be
68 linked with the spread of antibiotic resistance to human pathogens (Dodd 2012, Pruden 2014).
69 Mobile genetic elements carrying ARGs (e.g., plasmids, integrons, and transposons) can be
70 disseminated to and expressed by recipient cells through horizontal gene transfer (HGT),
71 including conjugation (mediated by cell to cell contact), transduction (bacteriophage mediated),
72 and transformation (mediated by extracellular DNA) (Lorenz and Wackernagel 1994) Of these,
73 transformation can be understood to represent the most basic mode of HGT, as it does not
74 require the presence of live donor cells or bacteriophages (Lorenz and Wackernagel 1994).
75 Consequently, quantification of the frequency with which an ARG in extracellular DNA can be
76 transported into and expressed by a recipient cell through transformation (hereafter referred to as
77 *transforming activity*) can provide a conservative measure of the ability of an ARG to undergo
78 HGT. Transforming activity encompasses (a) efficiency of extracellular DNA transport into a
79 recipient cell, (b) any repair of that DNA by the recipient cell in the event the DNA is damaged,
80 and (c) heritable incorporation and expression of the DNA's genetic information by recipient
81 cells, and is therefore a function of both the recipient cell's ability to import, repair, and express
82 a given ARG and the quality and quantity of the extracellular DNA containing the ARG.
83 Extracellular DNA can be released into the environment through secretion by live cells and lysis
84 of dead cells. While unstable to nucleases likely to be present in many aquatic matrixes, it can

85 persist in the environment through adsorption onto soil and sediments (Lorenz and Wackernagel
86 1994, Mao, Luo et al. 2014, Nagler, Insam et al. 2018).

87 Although conventional disinfection processes during water treatment (e.g., chlorine and UV)
88 efficiently inactivate ARB, intracellular ARGs are more difficult to degrade (McKinney and
89 Pruden 2012, Yoon, Chung et al. 2017, He, Zhou et al. 2019) and can be released into water
90 following the death of ARB cells (Zheng, Su et al. 2017). Sub-inhibitory concentrations of
91 disinfectants (e.g., chlorine and monochloramine) were even reported to promote the horizontal
92 transfer of ARGs by increasing the permeability of cell membrane and altering the expression of
93 conjugation-related genes (Guo, Yuan et al. 2015, Zhang, Gu et al. 2017). The proportion of
94 extracellular DNA carrying ARGs was found to increase after various biological and chemical
95 processes in wastewater treatment, revealing the potential risk of antibiotic resistance
96 dissemination in discharged effluent and receiving environments (Liu, Qu et al. 2018, Zhang, Li
97 et al. 2018). Previous studies have reported the enrichment of ARGs in surface water due to the
98 discharged effluents from upstream wastewater plants (Cacace, Fatta-Kassinos et al. 2019, Wu,
99 Su et al. 2019, Osińska, Korzeniewska et al. 2020). High diversity of ARGs in reclaimed
100 wastewater (e.g., agriculture irrigation, potable reuse) may pose risks of antibiotic resistance
101 dissemination to environmental bacteria and even human pathogens (Christou, Agüera et al.
102 2017, Hong, Julian et al. 2018).

103 UV-based advanced oxidation processes (UV-AOPs) are increasingly applied for the removal
104 of refractory contaminants during water treatment. The elimination of contaminants in UV-AOP
105 treatment is achieved by dual pathways, namely direct UV photolysis (depending on the UV
106 absorbances and quantum yields of target compounds) and oxidation by powerful radical species
107 (Stefan 2018). The activation of hydrogen peroxide (UV/H₂O₂) and peroxydisulfate (UV/S₂O₈²⁻)
108 by UV light produces hydroxyl radical (•OH) and sulfate radical (SO₄•⁻), respectively, which
109 can degrade a wide range of contaminants, as these two radicals react with many compounds at

110 or near diffusion-controlled reaction rates (Buxton, Greenstock et al. 1988, Neta, Huie et al.
111 1988).

112 UV/H₂O₂ and UV/S₂O₈²⁻ have also been reported to efficiently inactivate ARB cells
113 (Michael-Kordatou, Iacovou et al. 2015, Ferro, Guarino et al. 2016, Giannakis, Le et al. 2018).
114 However, detailed investigation into the reactivity of •OH with intracellular ARGs in these
115 studies was limited due to the significant consumption of •OH by constituents of the water
116 matrix and cell membranes before reaching the cell interiors (Ferro, Guarino et al. 2017, Yoon,
117 Chung et al. 2017, Zhang, Hu et al. 2019). Recent studies have reported that the reactivity of
118 •OH with extracellular chromosomal ARGs is highly dependent on the length of the monitored
119 ARG targets (He, Zhou et al. 2019). More studies are needed to assess whether the observed
120 reactivities are generally applicable to other types of DNA such as plasmid-encoded ARGs. To
121 the best of the authors' knowledge, little is known on the fate of ARGs during SO₄^{•-}-based
122 treatment processes.

123 Quantitative polymerase chain reaction (qPCR) has been widely applied to quantify
124 structurally-intact ARGs or to measure their degradation rates in water and wastewater treatment
125 (McKinney and Pruden 2012, Luby, Ibekwe et al. 2016, Hiller, Hübner et al. 2019). It should be
126 noted that qPCR methods usually record the degradation of a small fraction of a target ARG's
127 sequence length (with amplicon sizes typically <1000 bps), and not the entirety of a gene
128 (McKinney and Pruden 2012, Chang, Juhrend et al. 2017, Yoon, Dodd et al. 2018). In addition,
129 the efficiency of DNA replication (particularly of damaged DNA) in qPCR methods can be
130 different from that observed in bacterial cells subjected to transformation with the same DNA.
131 Furthermore, the uptake and repair of DNA by recipient cells can play important roles in
132 modulating gene transforming activity (Chang, Juhrend et al. 2017, Yoon, Dodd et al. 2018).
133 While the correlation between the degradation of target ARG amplicons (measured by qPCR)

134 and the elimination of ARG transforming activity was reasonably well explained for
135 chromosomal ARGs (He, Zhou et al. 2019), it is still less clear for plasmid-borne ARGs.

136 Exposure of DNA to UV and •OH is known to induce different types of DNA damage (von
137 Sonntag 2006). UV-C generates cyclobutane-pyrimidine dimers (CPDs) as the predominant
138 DNA lesions, while •OH can induce DNA damage ranging from base oxidation to phosphate-
139 sugar backbone breakages (Görner 1994, Sinha and Häder 2002, von Sonntag 2006). It is
140 currently not completely clear how the various type(s) of DNA damage resulting from UV, •OH,
141 and $\text{SO}_4^{\bullet-}$ are related to the deactivation of ARGs; for example, whether DNA lesions such as
142 CPDs (formed by direct UV irradiation) have the same effect on DNA transforming activity as
143 phosphate-sugar backbone breakage by •OH (generated by H_2O_2 or $\text{S}_2\text{O}_8^{2-}$ photolysis).
144 Furthermore, in UV-AOPs, DNA lesions can be generated by both direct UV irradiation and
145 radicals simultaneously.

146 The aim of this study was to investigate the fate of plasmid-encoded e-ARGs during the
147 common UV at 254 nm water disinfection process (UV_{254}) and its related AOPs. Plasmid
148 (pUC19) encoding an ampicillin resistance gene (amp^R) was purified from *Escherichia coli* (*E.*
149 *coli*) host cells and exposed to UV_{254} , to UV_{254} in combination with •OH or $\text{SO}_4^{\bullet-}$ (by using
150 $\text{UV}_{254}/\text{H}_2\text{O}_2$ and $\text{UV}_{254}/\text{S}_2\text{O}_8^{2-}$), or to •OH only (by combining UV at >290 nm with H_2O_2) (i.e.,
151 $\text{UV}_{>290}/\text{H}_2\text{O}_2$). $\text{UV}_{>290}/\text{H}_2\text{O}_2$ treatment was chosen to study the effect of •OH only exposure
152 because irradiation of H_2O_2 by $\text{UV}_{>290}$ can generate •OH, while neither $\text{UV}_{>290}$ irradiation nor
153 H_2O_2 directly affect amp^R under these experimental conditions (detailed in Section 3.1). The
154 treated plasmid samples were analysed by qPCR, gel electrophoresis, and ARG transformation
155 assay. DNA repair-proficient *E. coli* AB1157 (wild-type), as well as repair-deficient *E. coli*
156 mutants including AB1886 (uvrA^-), AB2463 (recA^-), AB2480 (uvrA^- , recA^-), and DH5 α
157 (recA^- , endA^-) were employed as recipient cells in the ARG transformation assay. Competition
158 kinetics methods using radical probe compounds were applied to measure the second-order rate

159 constants of $\bullet\text{OH}$ and $\text{SO}_4^{\bullet-}$ with *amp^R* segments. Experiments were also conducted in the
160 presence of wastewater effluent organic matter (EfOM) to study the effect of the dissolved
161 organic matter (DOM) on the removal of e-ARGs.

162 **2. Materials and Methods**

163 **2.1 Chemical Reagents**

164 All chemicals were in analytical grade or higher and used as received without further
165 purification. Ampicillin sodium salt (#A0166), agar powder (#A1296), sodium chloride
166 ($\geq 99.5\%$), *para*-chlorobenzoic acid (99%), and nitrobenzene ($\geq 99\%$) were purchased from
167 Sigma-Aldrich. Tryptone (#1612) and yeast extract (#1702) were supplied from Laboratorios
168 CONDA. Hydrogen peroxide 30% (Thermo Fisher Scientific) and sodium peroxydisulfate
169 ($\geq 98\%$, Sigma-Aldrich) were used to prepare the stock solutions of H_2O_2 and $\text{S}_2\text{O}_8^{2-}$,
170 respectively. All solutions were prepared in Milli-Q water (18 $\text{M}\Omega\cdot\text{cm}$, Millipore). EfOM was
171 previously extracted from the discharged effluent of a wastewater treatment plant in Jeddah,
172 Saudi-Arabia, with XAD resins (Zheng, Khan et al. 2014). Solutions of EfOM were prepared by
173 dissolving the hydrophobic and transphilic fractions (2:1 by mass) of EfOM in phosphate buffer.

174 **2.2 Plasmid Preparation**

175 Plasmid pUC19 was extracted from *E. coli* DH5 α . pUC19 (2686 bp) is a commercially
176 available *E. coli* vector carrying an ampicillin resistance gene (*amp^R*, 861 bp). One hundred μL
177 of *E. coli* DH5 α mid-exponential growth phase culture in LB broth medium with 50 mg/L of
178 ampicillin was transferred into 150 mL of LB broth medium containing 50 mg/L of ampicillin
179 and incubated overnight (200 rpm, 37°C). Plasmids were extracted from this overnight stock
180 solution using an AccuPrep Plasmid Mini Extraction kit (Bioneer 2016). The concentration of
181 recovered plasmid DNA was measured on a NanoDrop ND-2000 Spectrophotometer
182 (NanoDrop Products, Wilmington, USA).

183 2.3 UV Experiments

184 UV₂₅₄-based experiments were carried out with a UV quasi-collimated beam device equipped
185 with a low-pressure mercury lamp emitting UV light primarily at 254 nm (Sankyo Denki Ltd.,
186 Tokyo, Japan). The UV light was collimated onto the experimental solution, which was
187 contained in a petri dish placed on a magnetic stirrer. The average UV intensity (0.3 mW/cm²)
188 was determined with atrazine chemical actinometry (Lee, Gerrity et al. 2016). Experimental
189 solutions were prepared in autoclaved 2 mM phosphate buffer at pH 7. The initial concentration
190 of plasmid DNA used in experiments was 0.3 or 1 µg/mL. The applied UV fluences ranged from
191 0–180 mJ/cm². The initial concentrations of H₂O₂ and S₂O₈²⁻ were 0.5 mM for UV₂₅₄/H₂O₂ and
192 UV₂₅₄/S₂O₈²⁻, respectively. UV_{>290}/H₂O₂ experiments were conducted using a Model 66924 arc
193 lamp source fitted with a 450-W O₃-free Xe arc lamp and focusing collimator, and equipped
194 with an atmospheric attenuation filter and dichroic mirror to restrict lamp output to near-UV
195 wavelengths (290 nm < λ < 400 nm) (Newport-Oriel Model 66924; Stratford, CT). Relatively
196 high H₂O₂ concentrations (i.e., 10 mM) were applied for UV_{>290}/H₂O₂, in order to increase the
197 yield of •OH due to the low absorbance of UV light by H₂O₂ in this wavelength region. Samples
198 were withdrawn from the irradiated solutions in each experimental setup at predetermined time
199 intervals for DNA and probe compound analyses. Residual H₂O₂ and S₂O₈²⁻ were quenched
200 with excess bovine catalase and sodium thiosulfate, respectively. Samples for DNA analysis
201 (500 µL) were stored at -20°C and analysed within 24 h. Control experiments indicated that
202 H₂O₂ and S₂O₈²⁻ did not affect qPCR analyses within these experimental conditions (Figure S1).

203 2.4 Radical probe compounds

204 *para*-chlorobenzoic acid (*p*CBA) was used as •OH probe during UV₂₅₄/H₂O₂ and
205 UV_{>290}/H₂O₂ experiments. Both *p*CBA and nitrobenzene were applied during UV₂₅₄/S₂O₈²⁻.
206 Nitrobenzene can be used as a selective •OH probe compound ($k_{\bullet\text{OH}}=3.9\times 10^9 \text{ M}^{-1} \text{ s}^{-1}$) (Buxton,

207 Greenstock et al. 1988) due to its low reactivity to $\text{SO}_4^{\bullet-}$ ($k_{\text{SO}_4^{\bullet-}} < 10^6 \text{ M}^{-1} \text{ s}^{-1}$) (Neta, Madhavan et
208 al. 1977), whereas *p*CBA reacts with both radicals (i.e., $k_{\text{SO}_4^{\bullet-}} = 3.6 \times 10^8 \text{ M}^{-1} \text{ s}^{-1}$ and $k_{\bullet\text{OH}} = 5 \times 10^9$
209 $\text{M}^{-1} \text{ s}^{-1}$) (Neta, Madhavan et al. 1977, Buxton, Greenstock et al. 1988). *p*CBA and nitrobenzene
210 were analysed on a high-performance liquid chromatograph (HPLC, Dionex Ultimate 3000,
211 Thermo Scientific) equipped with an XDB-C18 column (5 μm , 4.6 \times 150 mm, Agilent). The
212 mobile phase comprised acetonitrile and 10 mM phosphoric acid (40:60, v/v). The two probe
213 compounds were analysed at their maximum absorbance wavelengths (i.e., 240 and 270 nm for
214 *p*CBA and nitrobenzene, respectively).

215 **2.5 qPCR Analysis**

216 Gene degradation was measured by qPCR using a CFX96 real-time PCR detection system
217 (Bio-Rad, Hercules, CA, USA). Four different amplicons (i.e., 192, 400, 603, and 851 bp) were
218 monitored, which covered varying fractions of *amp^R* as shown in Figure S2. The longest size of
219 *amp^R* segment targeted in qPCR was 851 bp instead of the whole *amp^R* gene (861 bp), due to the
220 low amplification efficiency of the 861 bp amplicon in the qPCR method. The reaction mixture
221 (20 μL) consisted of 1 μL of each primer, 1 μL of sample, 10 μL of EvaGreen® supermix, and 7
222 μL of autoclaved DNase free water. The qPCR protocol included one cycle at 95°C for 2 min,
223 30 cycles at 95°C for 5 s, an annealing step at 55°C for 60 s, and an elongation at 72°C for 20 s,
224 followed by a melt curve analysis from 65°C to 95°C. Each sample was analysed in triplicate.
225 More information on qPCR analysis, the DNA sequence of *amp^R*, and the monitored qPCR
226 target amplicons is described elsewhere (Yoon, Dodd et al. 2018).

227 **2.6 Gel Electrophoresis Analysis**

228 pUC19 plasmid (1 $\mu\text{g}/\text{mL}$) treated by UV_{254} and $\bullet\text{OH}$ ($\text{UV}_{>290}/\text{H}_2\text{O}_2$) was analysed by gel
229 electrophoresis to investigate the structural change of plasmid DNA. Linearized pUC19 was also
230 prepared for a reference by incubating the plasmid with type II restriction enzyme *EcoRI* (NEB,

231 USA) at 37 °C for 1 h, followed by enzyme inactivation at 65°C for 20 min. Plasmid samples
232 from UV₂₅₄, •OH (UV_{>290}/H₂O₂), and enzyme treatments, as well as a 1 kb DNA ladder
233 (Enzynomics, Korea) were loaded on 0.8% agarose gels at 4 V cm⁻¹ for 35 min. The bands were
234 visualized by ethidium bromide staining. Gel images were captured on a UV transilluminator
235 (Universal mutation detection system, UVP, LLC, USA).

236 **2.7 Gene Transformation Assays**

237 Non-ampicillin resistant *E.coli* K12 bacteria strains DH5α (*recA*⁻, *endA*⁻), AB1157 (wild-
238 type), AB1886 (*uvrA*⁻), AB2463 (*recA*⁻), and AB2480 (*uvrA*⁻, *recA*⁻) were used as recipient
239 cells for gene transformation assays. DH5α strain was commercially available from ATCC;
240 others were provided by CGSC (Coli Genetic Stock Center at Yale University). Details on
241 transformation assays were described by Yoon, Dodd et al. (2018). In brief, competent cells
242 were prepared by chemical treatment of non-resistant *E. coli* K12 strains using calcium chloride
243 and glycerol (Shanehbandi, Saei et al. 2013) and preserved at -80°C until use. Fifty μL of
244 treated plasmid sample was mixed with 100 μL of thawed competent cells. After incubating in
245 ice for 30 min, the mixture was quickly transferred onto a digital test tube heater (45°C) for 45 s
246 and then placed back in ice for 2 min. After the heat shock, the samples were mixed with 900
247 μL of LB broth and cultured for 45 min (200 rpm, 37°C). Finally, the incubated samples were
248 serially diluted with LB broth and plated onto two types of LB agar plates (i.e., with and without
249 inclusion of 50 mg/L of ampicillin). After 24 h of incubation at 37°C, the number of ARB
250 colonies (transformants) detected on selective agar plates (with ampicillin) were compared with
251 the total recipient cells growing on nonselective agar plates (without ampicillin). The gene
252 transformation efficiency was calculated as follows:

$$253 \quad \text{Transformation efficiency} = \frac{\text{Transformant cells}_{\text{selective plate}} \text{ (CFU/mL)}}{\text{Total recipient cells}_{\text{nonselective plate}} \text{ (CFU/mL)}}$$

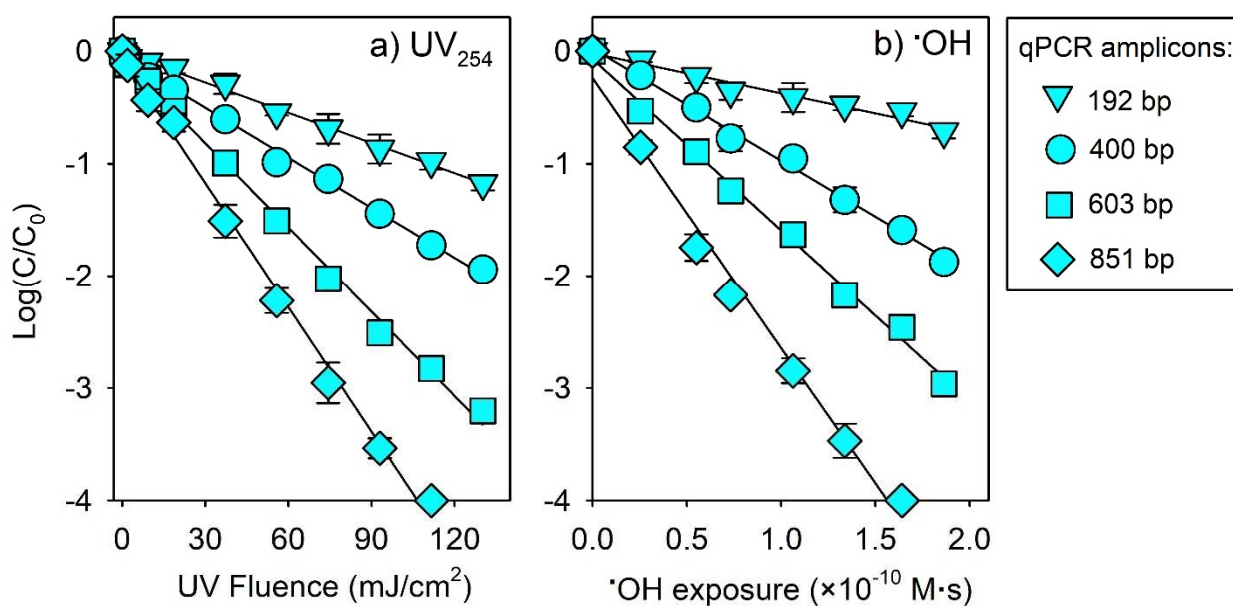
254 The typical concentrations of total recipient cells, as measured by culturing on nonselective agar
255 plates (without ampicillin), were approximately 3×10^8 and 2×10^8 CFU/mL for *E. coli* DH5 α and
256 *E. coli* AB strains, respectively. Control experiments conducted by directly plating the recipient
257 cells (without heat shock) on nonselective plates showed <10% variation in the final colony
258 counts of recipient cells as compared to the conditions incorporating heat shock (Figure S3), and
259 <50% variation in colony counts between strains. These results indicated that the type of
260 bacterial strain used, or stresses to which the strains were subjected during transformation assays
261 (e.g., heat shock), did not significantly impact the fitness or growth rates of recipient cells on
262 nonselective plates. Calibration curves prepared with known concentrations of plasmid DNA
263 indicated that the number of transformants linearly increased with increasing plasmid DNA
264 concentration from 10^{-5} – 10^{-1} μ g/mL (Figure S4). The transformation efficiency of *amp*^R
265 calculated for *E. coli* K12 strains was in the range of 10^{-4} – 10^{-8} , which was comparable with
266 previous studies (Chang, Juhrend et al. 2017, Yoon, Dodd et al. 2018).

267 **2.8 Statistical analysis**

268 Statistical analysis was conducted using SigmaPlot 12.0 and GraphPad Prism 7.0. The
269 fluence-based rate constants for gene degradation and transformation efficiency loss under
270 various experimental conditions were compared by multiple linear regression analysis. The null
271 hypothesis was that the first-order rate constants were identical, with $p=0.05$ as the threshold
272 significance level.

273 **3. Results and Discussions**

274 **3.1 e-ARG degradation during separate exposure to UV₂₅₄ and •OH**



275
 276 **Figure 1.** Degradation of *amp^R* segments during the treatment of pUC19 (1 μg/mL) with (a)
 277 UV₂₅₄ and (b) •OH (UV_{>290}/H₂O₂) at pH 7 (2 mM phosphate buffer). 10 mM of H₂O₂ and 1 μM
 278 of *pCBA* were added in UV_{>290}/H₂O₂ experiments. Error bars represent the standard deviations
 279 of triplicate experiments. Lines are the linear regressions of the experimental data.

280 *UV₂₅₄ exposure (Figure 1a).* The solution containing pUC19 was irradiated with UV₂₅₄ light
 281 (0–130 mJ/cm²). The degradation of *amp^R* segments (192, 400, 603, and 851 bp) measured by
 282 qPCR followed first-order kinetics with respect to UV fluence ($r^2 > 0.99$) (Figure 1a). The 192 bp
 283 *amp^R* segment was degraded by about 1-log at 110 mJ/cm², whereas 4-log reduction was already
 284 achieved for the 851 bp segment, which was close to the overall size of *amp^R* (861 bp). The
 285 resulting fluence-based rate constants derived from the slopes of linear curves, $k_{UV, Amp} = 2.303$
 286 × slope, are summarized in Table 1. The $k_{UV, Amp}$ of *amp^R* segments increased with amplicon
 287 size, which was consistent with the increasing number of potential reaction sites with increasing
 288 number of nucleotide bps. The $k_{UV, Amp}$ values obtained from this study were comparable to
 289 previously-reported values for the same *amp^R* segments (Yoon, Dodd et al. 2018). The
 290 $k_{UV, plasmid}$ of pUC19 plasmid could be estimated by extrapolating the $k_{UV, Amp}$ of each

291 segment to the entire plasmid (e.g., $k_{UV,plasmid}=k_{UV,192bp}\times\frac{2686\text{ bp}}{192\text{ bp}}$), based on an assumption
 292 that the UV reactivity per base pair is the same across the entire plasmid. The $k_{UV,plasmid}$ values
 293 estimated from the 192, 400, 603, and 851 bp amplicons were $2.9(\pm 0.06)\times 10^{-1}$, $2.3(\pm 0.04)\times 10^{-1}$,
 294 $2.6(\pm 0.05)\times 10^{-1}$, and $2.7(\pm 0.06)\times 10^{-1}$ cm²/mJ, respectively, yielding an average
 295 $k_{UV,plasmid}$ value of $2.6(\pm 0.05)\times 10^{-1}$ cm²/mJ (Table 1).

296 A theoretical approach was recently employed to estimate the photoreactivity of DNA (i.e.,
 297 formation rate of CPDs and 6,4-photoproducts) based on the molar absorption coefficients,
 298 quantum yields, and the number of 5'-bipyrimidine-3' doublets of a given DNA (Yoon, Dodd et
 299 al. 2018, He, Zhou et al. 2019). By applying this approach, the overall DNA lesion formation
 300 rate on pUC19 upon UV₂₅₄ exposure, $k_{all\ lesions}$, was calculated as 2.1×10^{-1} cm²/mJ (Text S1),
 301 which was close to the average $k_{UV,plasmid}$ (2.6×10^{-1} cm²/mJ) predicted from qPCR results as
 302 mentioned above.

303 **Table 1.** Apparent rate constants for the degradation of amp^R segments and pUC19 plasmid, and
 304 the elimination of gene transforming activity during UV₂₅₄ and •OH only treatments ^a

amp^R segments		pUC19 plasmid ^b		Loss of gene transformation	
#base pairs (bps)	k_{Amp}	$k_{plasmid}$	average	Recipient cells	$k_{transformation}$
UV ₂₅₄ (cm ² /mJ)					
192	$2.0(\pm 0.05)\times 10^{-2}$	$2.9(\pm 0.06)\times 10^{-1}$	$2.6(\pm 0.05)\times 10^{-1}$	DH5α	$6.5(\pm 0.21)\times 10^{-2}$
400	$3.4(\pm 0.07)\times 10^{-2}$	$2.3(\pm 0.04)\times 10^{-1}$		AB1157	$1.0(\pm 0.03)\times 10^{-1}$
603	$5.8(\pm 0.11)\times 10^{-2}$	$2.6(\pm 0.05)\times 10^{-1}$		AB1886	$2.4(\pm 0.06)\times 10^{-1}$
851	$8.9(\pm 0.16)\times 10^{-2}$	$2.7(\pm 0.06)\times 10^{-1}$		AB2463	$1.6(\pm 0.06)\times 10^{-1}$
•OH (UV _{>290} /H ₂ O ₂) (M ⁻¹ s ⁻¹)					
192	$8.1(\pm 0.69)\times 10^9$	$1.2(\pm 0.10)\times 10^{11}$	$1.5(\pm 0.07)\times 10^{11}$	DH5α	$2.7(\pm 0.05)\times 10^{10}$
400	$2.2(\pm 0.07)\times 10^{10}$	$1.5(\pm 0.05)\times 10^{11}$		AB1157	$4.1(\pm 0.14)\times 10^{10}$
603	$3.5(\pm 0.10)\times 10^{10}$	$1.6(\pm 0.04)\times 10^{11}$		AB1886	$6.5(\pm 0.18)\times 10^{10}$
851	$5.6(\pm 0.27)\times 10^{10}$	$1.8(\pm 0.08)\times 10^{11}$		AB2463	$8.2(\pm 0.23)\times 10^{10}$

^a Experimental conditions: pUC19: 1 μg/mL, 2 mM phosphate buffer at pH 7, fluence range for UV₂₅₄: 0–130 mJ/cm², 10 mM of H₂O₂ and 1 μM of pCBA were added in UV_{>290}/H₂O₂. The apparent rate constant values were reported in the form of Mean ± Standard Error.

^b The $k_{plasmid}$ values of pUC19 plasmid were estimated based on the k_{Amp} of amp^R

segments obtained from qPCR analyses (see Section 3.1 for details).

305
306 \bullet OH exposure (Figure 1b). Control experiments have confirmed that amp^R segments were
307 stable under $UV_{>290}$ irradiation alone (Figure S5), which was attributed to the low UV
308 absorbance of plasmid DNA above 290 nm. Moreover, 10 mM (340 mg/L) of H_2O_2 had
309 negligible effect on amp^R segment (Figure S1). Thus, $UV_{>290}/H_2O_2$ was applied to investigate
310 the influence of \bullet OH on the degradation of e-ARG. The \bullet OH exposure, $\int[\bullet OH]dt$, in the
311 $UV_{>290}/H_2O_2$ system was obtained by following the degradation of $pCBA$, which was
312 additionally added in the experimental solution. No $UV_{>290}$ direct photolysis of $pCBA$ was
313 observed in the absence of H_2O_2 (Figure S6). Thus, the \bullet OH exposure was calculated from
314
$$\int[\bullet OH] dt = -\frac{\ln\frac{[pCBA]}{[pCBA]_0}}{k_{\bullet OH,pCBA}}$$
 (Elovitz and von Gunten 1999), where the $k_{\bullet OH,pCBA}$ is the second-
315 order rate constant of \bullet OH with $pCBA$ ($5\times 10^9 M^{-1} s^{-1}$) (Buxton, Greenstock et al. 1988). The
316 logarithmic-scale degradation of amp^R segments exhibited linear correlations with \bullet OH exposure
317 during $UV_{>290}/H_2O_2$ (Figure 1b). The resulting bimolecular rate constants derived from the
318 slopes of linear curves, $k_{\bullet OH,Amp} = 2.303 \times \text{slope}$, are summarized in Table 1.

319 The $k_{\bullet OH,Amp}$ of amp^R segments increased with amplicon size, ranging from $8.1\times 10^9 M^{-1} s^{-1}$
320 for the 192 bp amplicon to $5.6\times 10^{10} M^{-1} s^{-1}$ for the 851 bp amplicon (Table 1). A good linear
321 relationship ($r^2=0.996$) was observed between the $k_{\bullet OH,Amp}$ and the base pair number of amp^R
322 segments (Figure S7), which was consistent with previous findings that \bullet OH non-selectively
323 reacts with all nucleotides in a DNA sequence (both AT and GC contents) (He, Zhou et al.
324 2019). The $k_{\bullet OH,plasmid}$ of the entire plasmid was predicted to be $1.8\times 10^{11} M^{-1} s^{-1}$ by applying
325 the base pair number of pUC19 (2686 bps) into the regression equation of this linear curve
326 (Figure S7). Alternatively, similar to the $k_{UV,plasmid}$ as mentioned above, the $k_{\bullet OH,plasmid}$ of

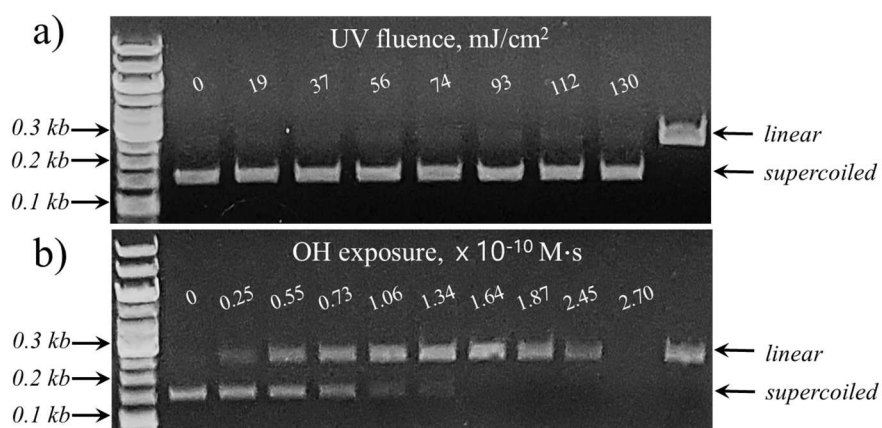
327 pUC19 was also estimated by normalizing the $k_{\bullet OH, Amp}$ of each segment (qPCR analyses) to the
328 entire plasmid and calculating the average value as $1.5(\pm 0.07) \times 10^{11} \text{ M}^{-1} \text{ s}^{-1}$ (Table 1).

329 The $k_{\bullet OH, Amp}$ values for the plasmid-encoded amp^R segments in this study were lower by a
330 factor of ~ 3 than those reported for the chromosome-encoded *blt* genes with similar amplicon
331 length (He, Zhou et al. 2019). To see whether the reactivity difference is due to the
332 conformational difference between the supercoiled-form plasmid and linear-form genomic DNA,
333 the theoretical diffusion-controlled rate constant for the reaction of $\bullet OH$ with supercoiled
334 pUC19 was calculated based on a method proposed by He, Zhou et al. (2019). The theoretical
335 maximum $k_{\bullet OH}$ value was predicted as $3.84 \times 10^{11} \text{ M}^{-1} \text{ s}^{-1}$ for pUC19, which yields a bp-specific
336 $k_{\bullet OH}$ value of $1.43 \times 10^8 \text{ M}_{AT+GC}^{-1} \text{ s}^{-1}$ when normalized to the length (in AT+GC bps) of pUC19
337 (2686 bps) (Text S2). For comparison, the theoretical maximum $k_{\bullet OH}$ value was $7.97 \times 10^{12} \text{ M}^{-1}$
338 s^{-1} for a hypothetical 50-kbp linear-form segment of genomic DNA, yielding a bp-specific $k_{\bullet OH}$
339 value of $1.59 \times 10^8 \text{ M}_{AT+GC}^{-1} \text{ s}^{-1}$ (He, Zhou et al. 2019). This indicates that the conformational
340 difference between the plasmid (supercoiled) and genomic (linear) DNA (the bp-specific $k_{\bullet OH}$
341 differed only by a factor of 1.1) does not explain the observed $\bullet OH$ reactivity difference. The
342 maximum $k_{\bullet OH}$ values for the amp^R amplicons can also be calculated by multiplying the bp-
343 specific $k_{\bullet OH}$ ($1.43 \times 10^8 \text{ M}_{AT+GC}^{-1} \text{ s}^{-1}$) with the length of each amplicon, and ranged from
344 $2.57 \times 10^{10} \text{ M}^{-1} \text{ s}^{-1}$ for 192 bp to $1.14 \times 10^{11} \text{ M}^{-1} \text{ s}^{-1}$ for 851 bp (Text S2). Thus, the experimental
345 $k_{\bullet OH, Amp}$ for pUC19 were lower by a factor of 2.5 than the theoretical maximum
346 $k_{\bullet OH, Amp}$ values. This difference is acceptable considering all possible experimental errors as
347 well as the hypothesis applied in the theoretical calculation.

348 *Structural degradation of plasmid (Figure 2)*. Figure 2a shows the electrophoresis gel of
349 pUC19 exposed to UV_{254} . The intact pUC19 before the UV_{254} exposure showed a band located
350 lower than the linearized pUC19 by *EcoRI*. Plasmid DNA generally exists in a supercoiled form,

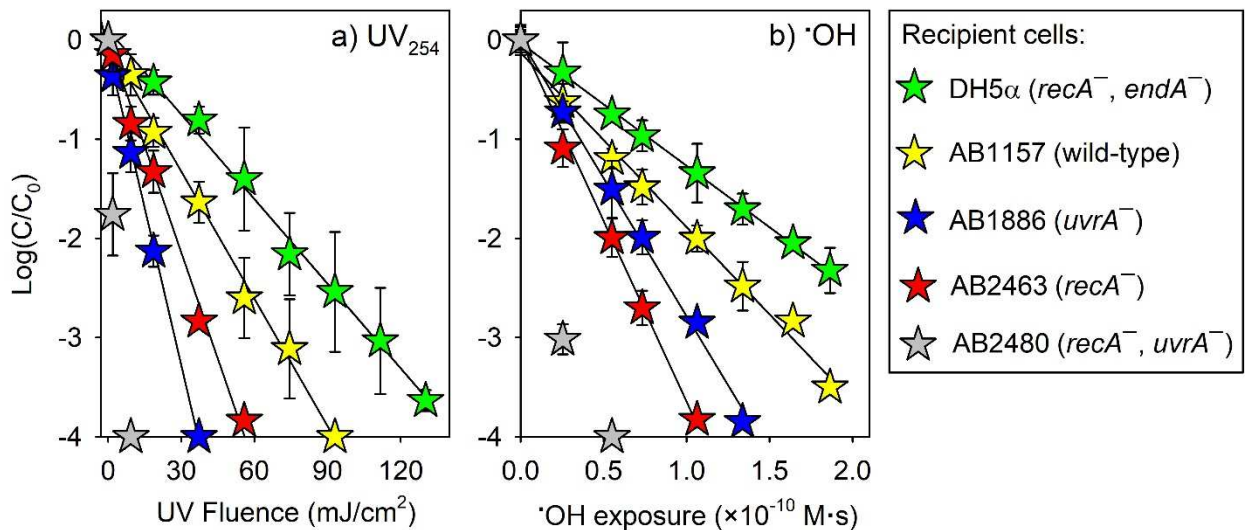
351 which is smaller than its linear form and migrates faster in electrophoresis gel. The UV₂₅₄
 352 irradiation (0–130 mJ/cm²) did not change the position of the band, suggesting that the pUC19
 353 kept its supercoiled form without significant conformational change (e.g., strand breakage). It is
 354 well documented that the gene damage by UV₂₅₄ is mainly caused by the formation of DNA
 355 lesions such as CPDs and 6,4-photoproducts (pyrimidine adducts) (Siřha and Hader 2002, Cadet
 356 and Douki 2018), which are generally not detectable by gel electrophoresis analysis (Yoo,
 357 Dodd et al. 2018).

358 The reaction pathways of •OH with DNA include addition to nucleobases – producing adduct
 359 radicals – and hydrogen-abstraction from 2-deoxyribose (sugar moiety) (von Sonntag 2006,
 360 Dizdaroglu and Jaruga 2012), resulting in not only oxidized bases and abasic sites, but also
 361 strand breaks (Cadet, Delatour et al. 1999, von Sonntag 2006). The double-strand breaks are
 362 expected to be mainly responsible for the conformational change from supercoiled to linear
 363 plasmid form. Gel electrophoresis analysis showed that the pUC19 plasmid band gradually
 364 moved from the supercoiled to linear form position with increasing •OH exposure (Figure 2b),
 365 revealing the formation of double-strand breaks in pUC19.



366
 367 **Figure 2.** DNA electrophoresis gel of pUC19 treated by (a) UV₂₅₄ and (b) •OH (UV_{>290}/H₂O₂).
 368 First column shows the standard DNA ladders. Last column shows the linearized pUC19 after
 369 treating with *EcoRI* restriction digestion.

370 **3.2 e-ARG deactivation (loss of transforming activity) during separate exposure to UV₂₅₄**
 371 **and •OH**



373 **Figure 3.** Elimination of gene transforming activity during the treatment of pUC19 (1 µg/mL)
 374 with (a) UV₂₅₄ and (b) •OH (UV_{>290}/H₂O₂) at pH 7 (2 mM phosphate buffer). 10 mM of H₂O₂
 375 and 1 µM of *pCBA* were added in UV_{>290}/H₂O₂ experiments. The parentheses in legend show
 376 the deficient DNA repair genes in recipient cells. Error bars represent the standard deviations of
 377 triplicate experiments. Lines are the linear regressions of the experimental data.

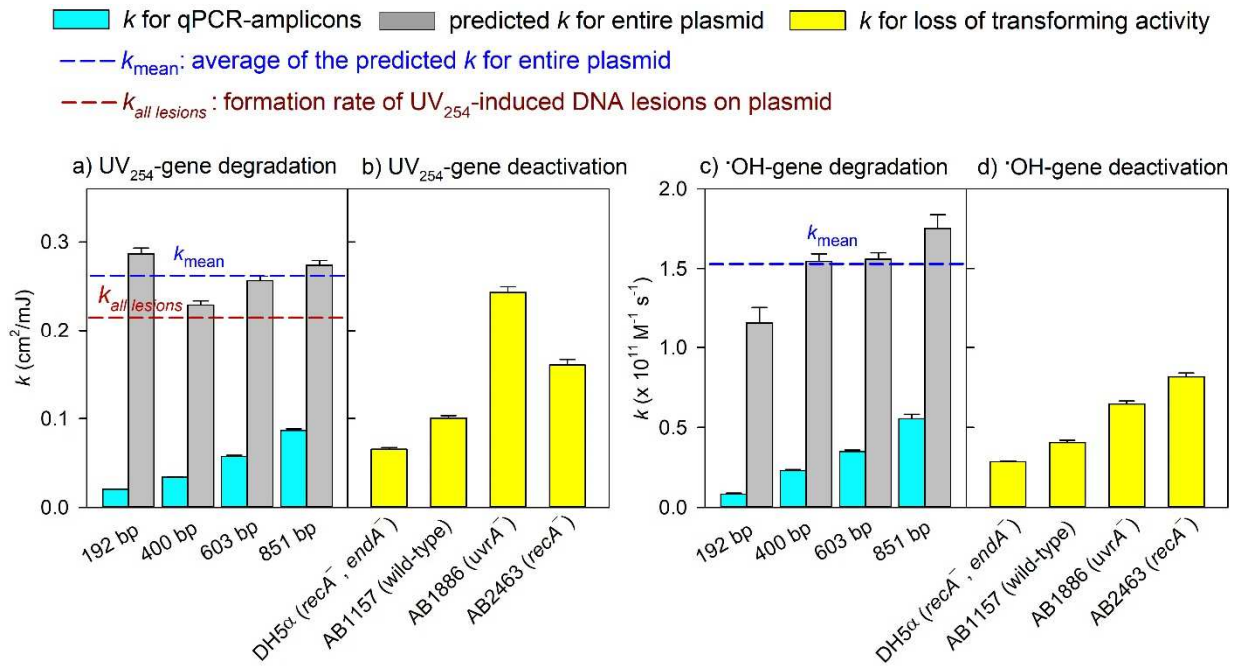
378 Bacterial cells have developed the ability of repairing DNA lesions induced by UV
 379 irradiation and oxidant stress (e.g., radicals) using several enzyme systems (Teebor, Boorstein et
 380 al. 1988, Sinha and Häder 2002). The biological deactivation of pUC19 upon separate treatment
 381 with UV₂₅₄ and •OH was studied by analysing its transformation of non-resistant recipient cells
 382 having different DNA repair abilities. The decrease of transforming activity of pUC19 followed
 383 first-order kinetics with respect to UV fluence or •OH exposure, and was variable depending on
 384 the recipient cells used (Figure 3). The most rapid decrease was observed for AB2480 (*uvrA*⁻,
 385 *recA*⁻) during each separate treatment with UV₂₅₄ and •OH. No transformant was detectable
 386 from AB2480 (more than 4-log decrease) when the UV fluence was above 5 mJ/cm², or when

387 the $\bullet\text{OH}$ exposure was higher than 5.5×10^{-11} M·s. Thus, the fluence-based rate constant for UV
388 ($k_{UV,transformation}$) and second-order rate constant for $\bullet\text{OH}$ ($k_{\bullet\text{OH},transformation}$) for the
389 transforming activity loss for AB2480 were not calculated in this case due to the limited data
390 points.

391 During UV₂₅₄ exposure (Figure 3a), the loss of transforming activity was slower in AB1886
392 (*uvrA*⁻, 0.24 cm²/mJ) than AB2480, followed by AB2463 (*recA*⁻, 0.16 cm²/mJ), AB1157 (wild-
393 type, 0.10 cm²/mJ), and DH5 α (*recA*⁻, *endA*⁻, 0.07 cm²/mJ), in which the values in parentheses
394 show $k_{UV,transformation}$ (Table 1). The variation in the transformation efficiency of plasmids
395 carrying the same DNA damage indicated that the UV-induced damage can be repaired by
396 recipient cells to different extents, depending on their repair gene proficiencies (or deficiencies).
397 The *uvrABC* proteins involve the nucleotide excision repair of a variety of DNA lesions
398 including the UV-induced CPDs and 6,4-photoproducts. This process is initiated by the
399 interaction of *uvrA* protein with DNA to recognize the damaged sites (Kisker, Kuper et al.
400 2013). The *recA* protein is essential for the post-replication repair of double-strand breaks and
401 single-strand gaps (e.g., T-T dimers) by homologous recombination (Smith and Wang 1989,
402 Shinohara and Ogawa 1995). These roles of *uvrA* and *recA* proteins well explained the trend
403 observed from the transformation rates of *E. coli* strains. AB2480 was most sensitive to UV-
404 induced DNA damage on pUC19 due to lack of both *uvrA* and *recA* genes. The *uvrA* deficient
405 AB1886 was the second most sensitive, followed by the *recA* deficient AB2463, indicating that
406 *uvrA* played a more important role than *recA* for the repair of UV-induced DNA damage. The
407 wild-type AB1157 was less sensitive than the other three *E. coli* mutant strains owing to its
408 DNA repair capability by *uvrA* and *recA*. Interestingly, despite its deficiency in *recA*, the DH5 α
409 strain exhibited even lower sensitivity to UV-induced DNA damage compared to wild-type
410 AB1157. This was possibly attributable to the lack of a functional *endA* gene in DH5 α . The
411 *endA* gene is associated with the formation of extracellular DNase I, which can hydrolyze

412 exogenous plasmid DNA, consequently reducing its uptake and transformation (Shou, Kang et
413 al. 2019). In line with this, the DH5 α showed ~10-fold higher transformation efficiency than the
414 other *E. coli* strains proficient in *endA* when all were transformed with equivalent concentrations
415 of undamaged pUC19 (Figure S4). This *endA* deficiency might therefore render *E. coli* DH5 α
416 inherently more active for DNA damage repair than the other strains, despite its lack of *recA*.

417 During \bullet OH exposure (Figure 3b), the rate of transforming activity loss was the highest for
418 AB2480 followed by AB2463 (*recA*⁻, $8.2 \times 10^{10} \text{ M}^{-1} \text{ s}^{-1}$), AB1886 (*uvrA*⁻, $6.5 \times 10^{10} \text{ M}^{-1} \text{ s}^{-1}$),
419 AB1157 (wild-type, $4.1 \times 10^{10} \text{ M}^{-1} \text{ s}^{-1}$), and DH5 α (*recA*⁻, *endA*⁻, $2.9 \times 10^{10} \text{ M}^{-1} \text{ s}^{-1}$) in which the
420 values in parentheses show $k_{\bullet\text{OH},\text{transformation}}$ (Table 1). The *recA* deficient AB2463 showed
421 higher sensitivity to \bullet OH-induced DNA damage than the *uvrA* deficient AB1886, which was
422 opposite compared to the case for UV₂₅₄ (Figure 3a). This suggests that *recA* is more efficient
423 for repairing \bullet OH-induced DNA damage, as homologous recombination is based on exchange of
424 (damaged) nucleotide sequences (Alberts, Johnson et al. 2002) and capable of repairing not only
425 base oxidation but also double-strand breaks. In contrast, *uvrA* is based on nucleotide excision
426 repair and more specific to the repair of UV-induced DNA lesions (base modification such as
427 CPDs), but not efficient for double-strand breaks (Alberts, Johnson et al. 2002).



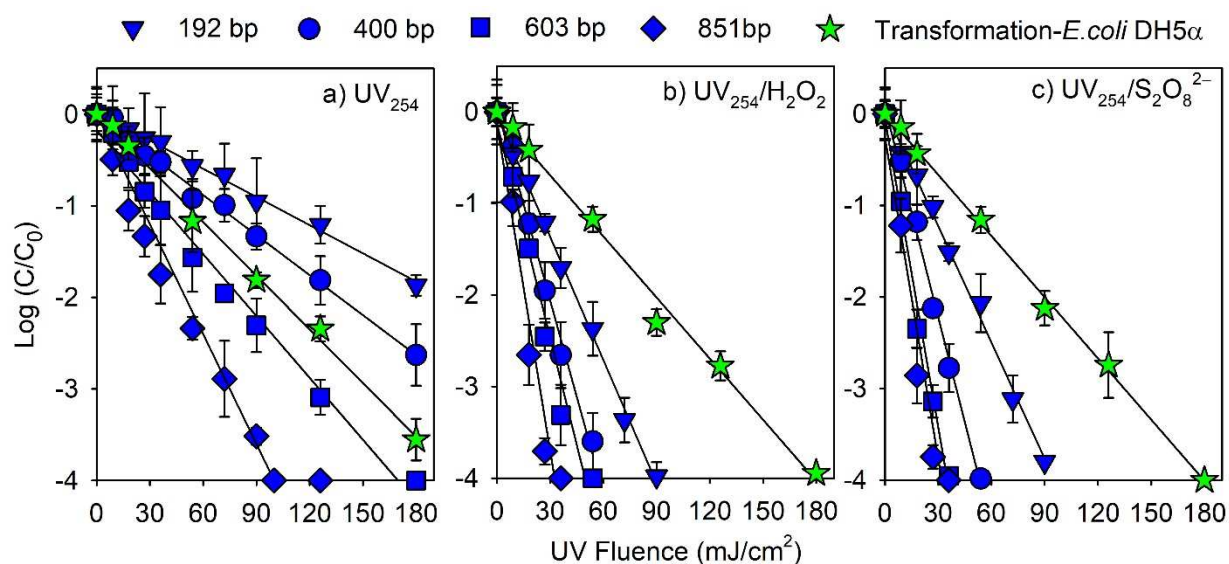
428

429 **Figure 4.** Apparent rate constants for the degradation of amp^R segments, pUC19 plasmid, and
 430 the elimination of gene transforming activity during exposure to (a, b) UV_{254} and (c, d) $\bullet\text{OH}$
 431 ($\text{UV}_{>290}/\text{H}_2\text{O}_2$). Specific kinetic parameters are summarized in Table 1 and error bars represent
 432 the standard errors of apparent rate constants. Rate constants for the loss of transforming activity
 433 in AB2480 were not calculated due to the limited data points.

434 The apparent rate constants for the degradation of amp^R segments, pUC19 plasmid, and the
 435 loss of gene transforming activity are compared in Figure 4. For both UV_{254} direct photolysis
 436 and $\bullet\text{OH}$ oxidation, the estimated degradation rates of the entire plasmid (based on qPCR
 437 analyses) overestimated the rates of pUC19 deactivation (loss of transforming activity) observed
 438 for all repair-proficient *E. coli* recipient strains, which can be explained by the repair of UV_{254} -
 439 and $\bullet\text{OH}$ -induced damage by repair-proficient recipient cells. Our results were in agreement
 440 with previous findings on the UV_{254} treated pWH1266 plasmid and its transformation of
 441 *Acinetobacter baylyi* (Chang, Juhrend et al. 2017). However, the rate of gene deactivation
 442 during UV_{254} direct photolysis measured using *uvrA* deficient AB1886 as the recipient strain
 443 was close to the estimated degradation rate of pUC19 and the formation rate of DNA lesions

444 (Figure 4a, b). The minimum rates of gene deactivation measured by double mutant AB2480
 445 (*uvrA*⁻, *recA*⁻) were estimated based on the limited data points shown in Figure 3, which gave
 446 0.91 cm²/mJ and 1.7×10¹¹ M⁻¹ s⁻¹ for UV₂₅₄ and •OH exposure, respectively. These values were
 447 significantly larger than the gene deactivation rates measured by any of the repair proficient
 448 strains. Furthermore, the degradation rate of the entire plasmid underestimated the loss of
 449 pUC19 transforming activity measured by AB2480 (*uvrA*⁻, *recA*⁻) during UV₂₅₄ direct
 450 photolysis and •OH oxidation.

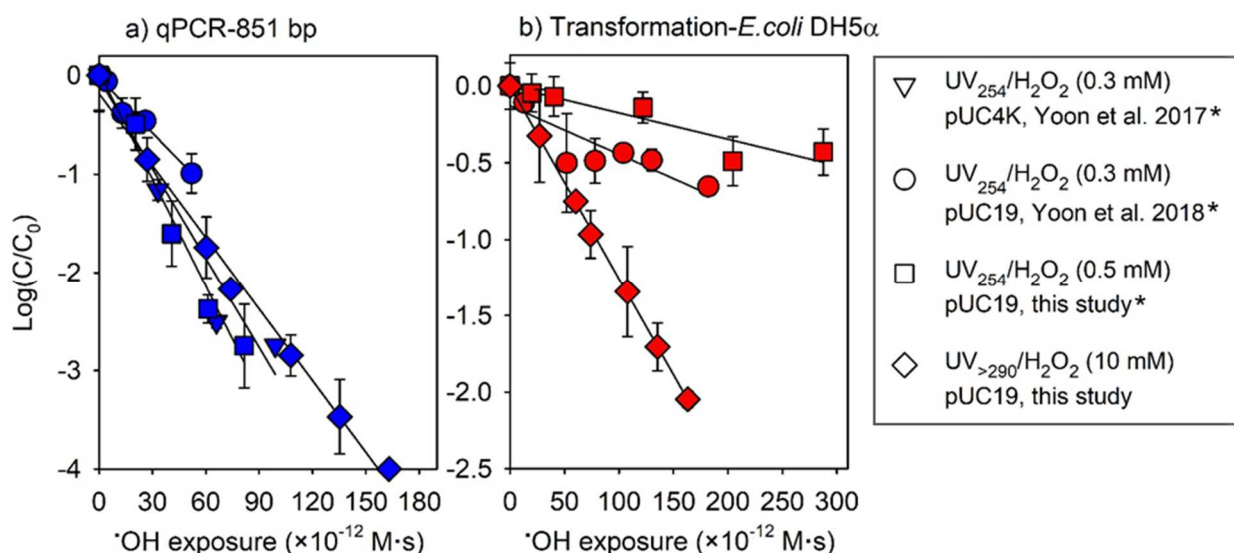
451 3.3 e-ARG degradation and deactivation by combined exposure to UV₂₅₄ and radicals



452 **Figure 5.** Degradation of *amp*^R segments and elimination of gene transforming activity (*E. coli*
 453 DH5α as recipient cells) with increasing UV fluence (0–180 mJ/cm²) during treatment of
 454 pUC19 (0.3 μg/mL) with (a) UV₂₅₄, (b) UV₂₅₄/H₂O₂ (0.5 mM), and (c) UV₂₅₄/S₂O₈²⁻ (0.5 mM)
 455 at pH 7 (2 mM phosphate buffer). *p*CBA (1 μM) was added in UV₂₅₄/H₂O₂ experiments for the
 456 quantification of •OH, and both *p*CBA and nitrobenzene (each 1 μM) were added in UV/S₂O₈²⁻
 457 experiments for the quantification of •OH and SO₄^{•-}. Error bars represent the standard
 458 deviations of triplicate experiments. Lines represent the linear regressions of experimental data.

460 The degradation of *amp^R* and the elimination of gene transforming activity (*E. coli* DH5 α as
461 recipient cells) were tested during combined exposure to UV₂₅₄ and radicals (\bullet OH and SO₄ \bullet^-), in
462 comparison to UV₂₅₄ direct photolysis. The degradation of *amp^R* amplicons followed first-order
463 kinetics with respect to UV fluence ($r^2 > 0.99$) during UV₂₅₄, UV₂₅₄/H₂O₂, and UV₂₅₄/S₂O₈²⁻
464 treatments (Figure 5). A lower initial concentration of pUC19 (0.3 μ g/mL) and a higher fluence
465 range (0–180 mJ/cm²) were applied in these tests than in the experiments described in the
466 preceding sections. However, the degradation rate constants of *amp^R* amplicons upon UV₂₅₄
467 direct photolysis (i.e., 2.4×10^{-2} – 8.2×10^{-2} cm²/mJ) (Table S1) were in good agreement with
468 those obtained during the treatment of 1 μ g/mL of pUC19 by 0–130 mJ/cm² of UV₂₅₄ (i.e.,
469 2.0×10^{-2} – 8.9×10^{-2} cm²/mJ, Table 1). The k_{UV_{254}/H_2O_2} of *amp^R* amplicons during UV₂₅₄/H₂O₂
470 were in the range of 1.0×10^{-1} – 3.0×10^{-1} cm²/mJ, which were larger than the $k_{UV_{254}}$ by a factor of
471 ~ 4 (Table S1). Therefore, the contribution of UV₂₅₄ direct photolysis to the overall gene
472 degradation during UV₂₅₄/H₂O₂ was only about 25% ($k_{UV_{254}}/k_{UV_{254}/H_2O_2} \times 100\%$), revealing
473 the significant role of \bullet OH exposure (75%).

474 The k_{UV_{254}/H_2O_2} for the elimination of gene transforming activity was $(5.1 \pm 0.2) \times 10^{-2}$ cm²/mJ,
475 which was larger than the $k_{UV_{254}}$ by a factor of only 1.1 ($k_{UV_{254}/H_2O_2}/k_{UV_{254}} = 1.1$, Table S1).
476 Thus, even though the \bullet OH exposure significantly accelerated gene degradation (by a factor of
477 4), its contribution to the elimination of gene transforming activity was not as efficient as
478 expected.



479
 480 **Figure 6.** (a) Degradation of amp^R segment (851 bp) and (b) elimination of gene transforming
 481 activity (*E. coli* DH5 α as recipient cells) as a function of $\bullet\text{OH}$ exposure during UV/H $_2\text{O}_2$
 482 treatments at different UV (254 nm and >290 nm) and H $_2\text{O}_2$ (0.3 mM, 0.5 mM, and 10 mM)
 483 conditions. The gene transforming activity was not measured in the study of Yoon et al. 2017
 484 for treating pUC4k with $\text{UV}_{254}/\text{H}_2\text{O}_2$ (0.3 mM). The values for the data sets designated by (*)
 485 represent contributions from $\bullet\text{OH}$ exposure only (estimated by subtracting UV_{254} contributions
 486 from overall measurements of qPCR signal or transforming activity loss). Error bars represent
 487 the standard deviations of triplicate experiments. Lines represent the linear regressions of
 488 experimental data.

489 Figure 6 summarizes the results from this study and the literature on the effect of $\bullet\text{OH}$
 490 exposure on degradation of the 851 bp amp^R segment and loss of gene transforming activity
 491 (measured using *E. coli* DH5 α as recipient strain). Plasmid pUC4k or pUC19 carrying amp^R
 492 was treated with UV/H $_2\text{O}_2$ at different conditions of UV wavelength and initial H $_2\text{O}_2$
 493 concentrations, i.e., $\text{UV}_{254}/\text{H}_2\text{O}_2$ (0.3 mM or 0.5 mM) and $\text{UV}_{>290}/\text{H}_2\text{O}_2$ (10 mM). The $\bullet\text{OH}$ -
 494 induced degradation or deactivation were calculated by subtracting the effect of UV_{254} direct
 495 photolysis from the overall results of corresponding $\text{UV}_{254}/\text{H}_2\text{O}_2$. Although the statistical
 496 analysis showed a significant variation ($p=0.0149$) in the slopes of linear curves in Figure 6a,

497 the $k_{\bullet OH, 851 bp}$ values during UV₂₅₄/H₂O₂ treatment differed only by factors of 0.8–1.5 from that
498 during $\bullet OH$ only process (UV_{>290}/H₂O₂). This suggested that UV₂₅₄-induced gene damage on the
499 plasmid (e.g., CPDs and pyrimidine adducts) did not cause significant impact on the reactivity
500 of $\bullet OH$ with nucleobase and sugar moieties during UV₂₅₄/H₂O₂. However, the elimination of
501 gene transforming activity (measured using *E. coli* DH5 α as recipient strain) varied significantly
502 in the different treatments. The loss of gene transforming activity was ~5 times slower in
503 UV₂₅₄/H₂O₂ processes (UV₂₅₄ and $\bullet OH$ co-exist) as compared to that obtained from
504 UV_{>290}/H₂O₂ ($\bullet OH$ only). This indicates that the elimination of gene transforming activity
505 caused by UV₂₅₄ direct photolysis and $\bullet OH$ oxidation were not additive during UV₂₅₄/H₂O₂. One
506 possible explanation could be that some DNA damage repair pathways such as nucleotide
507 excision repair by *uvrABC* also repaired $\bullet OH$ -induced lesions (e.g., base oxidation) located near
508 the UV-induced lesions, leading to much less extensive loss of transforming activity than would
509 be expected from simple summation of the losses in transforming activity observed for UV₂₅₄
510 and $\bullet OH$ exposure separately.

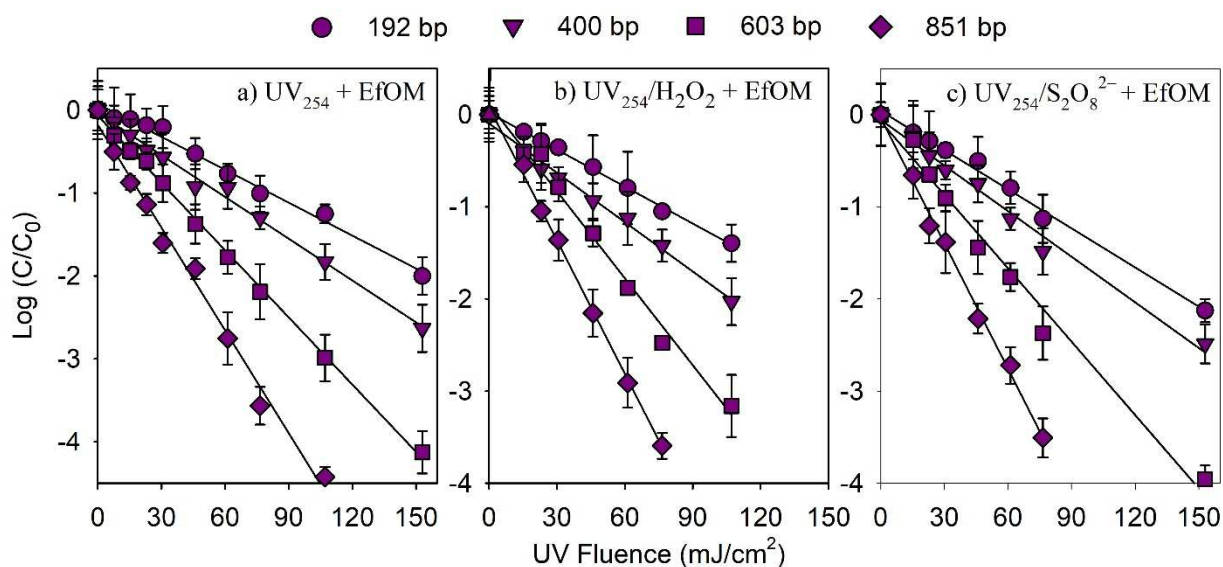
511 The degradation rates of *amp*^R amplicons (1.0×10^{-1} – 3.2×10^{-1} cm²/mJ) during UV₂₅₄/S₂O₈²⁻
512 were also ~4-fold larger than that obtained during UV₂₅₄ (Table S1). SO₄^{•-} is the primary radical
513 generated during UV₂₅₄ photolysis of S₂O₈²⁻. However, SO₄^{•-} can further react with H₂O, OH⁻,
514 and Cl⁻ (sometimes present as an impurity) in aqueous solution to produce $\bullet OH$ (Lutze, Kerlin
515 et al. 2015). Using the degradation kinetics of radical probe compounds (nitrobenzene and
516 *p*CBA) (Figures S7 and S8), the steady-state concentration of $\bullet OH$ during UV₂₅₄/S₂O₈²⁻ was
517 determined to be 6.4×10^{-13} M, which was approximately two orders of magnitude smaller than
518 that of SO₄^{•-} (1.8×10^{-11} M) under experimental conditions used here (Text S3). This was
519 consistent with the theoretically estimated values considering all the possible reactions related to
520 $\bullet OH$ formation in UV₂₅₄/S₂O₈²⁻ system (Text S4). Despite the much lower concentration, the
521 contribution of $\bullet OH$ to the overall gene damage cannot be ignored, as the *amp*^R segments

522 appeared to be much more reactive to •OH than SO₄•⁻ (see discussions below). Thus, the
523 percentages of gene degradation attributable to UV₂₅₄ direct photolysis, SO₄•⁻, and •OH during
524 UV₂₅₄/S₂O₈²⁻ treatment could be estimated as ~23%, ~33%, and ~44%, respectively, in which
525 the relative contributions of each pathway to the overall gene damage were calculated based on
526 the observed rate constants for degradation of *amp*^R amplicons during UV₂₅₄ and
527 UV₂₅₄/S₂O₈²⁻ treatments, the steady-state concentrations of •OH and SO₄•⁻ in UV₂₅₄/S₂O₈²⁻
528 experiments, and the second-order rate constants for reactions of •OH and SO₄•⁻ with the *amp*^R
529 amplicons (Text S5).

530 The second-order rate constants of SO₄•⁻ with *amp*^R segments were determined to be in the
531 range of (1.07–1.96)×10⁹ M⁻¹ s⁻¹ (Text S5 and Table S2), which were about an order of
532 magnitude lower than the •OH rate constants (Table 1). SO₄•⁻ preferentially adds to the electron-
533 rich sites of the nucleobases (e.g., C₅ of pyrimidines) to generate radical adducts, which decay to
534 nucleobase radicals as intermediates, followed by hydroxylation and oxidation in aqueous
535 solution (von Sonntag 2006). However, SO₄•⁻ is larger than •OH and negatively charged.
536 Therefore, steric hindrance and electrostatic repulsion might decrease the reactivity of SO₄•⁻
537 toward negatively charged DNA molecules in comparison to •OH.

538 Similar to UV₂₅₄/H₂O₂ processes, the elimination rate of pUC19 transforming activity during
539 UV₂₅₄/S₂O₈²⁻ treatment was also only slightly larger than that in UV₂₅₄ direct photolysis
540 ($k_{UV_{254}/S_2O_8^{2-}}/k_{UV_{254}} = 1.1$, Table S1), even while the observed amplicon *degradation* rates
541 were ~4-fold faster for UV₂₅₄/S₂O₈²⁻ compared to UV₂₅₄ direct photolysis. This further supports
542 the above findings that co-exposure to UV₂₅₄ and radicals during UV₂₅₄-AOPs did not lead to
543 faster transforming activity loss than the separate exposures to UV₂₅₄ and radicals, due to the
544 facile repair of UV₂₅₄ and/or radical-induced DNA damage in host cells.

545 **3.5 Effect of wastewater effluent organic matter on the degradation of *amp^R* during UV₂₅₄-**
 546 **AOPs**



547
 548 **Figure 7.** Degradation of *amp^R* segments in the presence of wastewater effluent organic matter
 549 (5.4 mg C/L) during the treatment of pUC19 (0.31 µg/mL) with (a) UV₂₅₄, (b) UV₂₅₄/H₂O₂ (0.5
 550 mM), and (c) UV₂₅₄/S₂O₈²⁻ (0.5 mM) at pH 7 (2 mM phosphate buffer). *p*CBA (1 µM) was
 551 added in UV₂₅₄/H₂O₂ experiments for the quantification of •OH, and both *p*CBA and
 552 nitrobenzene (each 1 µM) were added in UV/S₂O₈²⁻ experiments for the quantification of •OH
 553 and SO₄^{•-}. Error bars represent the standard deviations of triplicate experiments. Lines represent
 554 the linear regressions of experimental data.

555 The efficiencies of *amp^R* degradation during UV₂₅₄, UV₂₅₄/H₂O₂, and UV₂₅₄/S₂O₈²⁻
 556 experiments were investigated in the presence of EfOM (5.4 mg C/L). The UV 254 nm
 557 absorbance of EfOM solution (*a*₂₅₄) was 0.1 cm⁻¹. The path length in the petri dish (*L*) was 1.6
 558 cm. Thus, the water factor, $WF = (1 - 10^{-a_{254} \cdot L}) / (a_{254} \cdot L \cdot \ln 10)$ (Bolton and Linden 2003), was
 559 calculated to be 0.84. The average UV intensity in the solution containing EfOM was then
 560 corrected from 0.30 mW/cm² to 0.25 mW/cm² using the calculated water factor (Lee, Gerrity et
 561 al. 2016). The *amp^R* segments were gradually degraded with increasing UV fluence following

562 first-order kinetics (Figure 7). Interestingly, the $k_{UV,Amp}$ of each segment during UV₂₅₄
563 irradiation in the presence of EfOM was approximately 1.2 times higher than the corresponding
564 conditions without EfOM ($p < 0.0001$) (Table S1). Chromophoric dissolved organic matter
565 (DOM) is known to generate reactive species upon UV irradiation, such as triplet excited states
566 of DOM (³DOM*), singlet oxygen, and •OH, which have been proven to contribute to the
567 oxidation of organic pollutants (Chin, Miller et al. 2004, Lester, Sharpless et al. 2013, Batista,
568 Teixeira et al. 2016, Rosario-Ortiz and Canonica 2016). Bacteriophage MS2 was found to be
569 inactivated by ³DOM* and singlet oxygen generated from sunlight irradiation of wastewater and
570 river water DOM isolates (Kohn, Grandbois et al. 2007, Kohn and Nelson 2007, Rosado-Lausell,
571 Wang et al. 2013). The reactive oxygen species (e.g., singlet oxygen, superoxide, H₂O₂)
572 generated during photooxidations involving ³DOM* were proposed to inactivate bacteria by
573 damaging DNA, proteins, and cell membranes (Song, Mohseni et al. 2016, Nelson, Boehm et al.
574 2018). Our findings suggest that through its photosensitizing properties, DOM can indirectly
575 contribute to the photodegradation of e-ARGs. Similar results were reported recently on the
576 enhanced photo-degradation of pBR322 plasmid-encoded *tet A* and *bla_{TEM-1}* genes in DOM
577 solution (Zhang, Li et al. 2019). This degradation pathway might play an especially important
578 role during solar disinfection processes, due to the low UV absorbance characteristics of DNA at
579 high wavelengths (and consequent minimal direct UV photolysis under such conditions).

580 In contrast, EfOM mainly acted as radical scavenger during UV₂₅₄/H₂O₂ and UV₂₅₄/S₂O₈²⁻
581 experiments. The k_{UV_{254}/H_2O_2} and $k_{UV_{254}/S_2O_8^{2-}}$ of *amp^R* segments in the presence of EfOM were
582 each decreased by a factor of ~3 compared to the conditions without EfOM (Table S1). The
583 degradation kinetics of *pCBA* and nitrobenzene (Figure S10) also confirmed the much lower
584 levels of radicals in the presence of EfOM (e.g., [SO₄•⁻]_{ss}: 9.5×10⁻¹³ M with EfOM vs. 1.8×10⁻¹¹
585 M without EfOM). Overall, the degradation efficiency of *amp^R* in the presence of EfOM

586 increased only marginally (within a factor of 1.4) during UV₂₅₄/H₂O₂ and UV₂₅₄/S₂O₈²⁻,
587 compared to UV₂₅₄ alone, due to the significant scavenging of radicals by EfOM.

588 4. Conclusions

- 589 • The degradation of *amp^R* segments and the loss of gene transforming activity followed first-
590 order kinetics with respect to UV fluence and •OH exposure during UV₂₅₄ direct photolysis
591 and •OH oxidation (UV_{>290}/H₂O₂). The degradation rate constants of *amp^R* segments
592 increased with amplicon size, which corresponded to the increase in nucleotide bps (and
593 hence, reaction sites) with increased amplicon length. Gel electrophoresis results indicated
594 that UV₂₅₄ (0–130 mJ/cm²) did not change the supercoiled conformation of pUC19 plasmid,
595 whereas •OH exposure (0–2.7×10⁻¹⁰ M·s) led to strand-breaks.
- 596 • The loss of gene transforming activity varied depending on the type of recipient cells.
597 Double mutant AB2480, which was deficient in repair genes *uvrA* and *recA*, was the most
598 sensitive to DNA damage induced by UV₂₅₄ direct photolysis and •OH oxidation. The
599 predicted degradation rates for the entire pUC19 plasmid overestimated the loss in
600 transforming activity of pUC19 for all recipient cells other than AB2480, apparently due to
601 the repair of DNA damage by repair-proficient strains.
- 602 • The second-order rate constants of •OH with *amp^R* segments were determined to be in the
603 range of 8.1×10⁹ – 5.6×10¹⁰ (M⁻¹ s⁻¹) and showed a strong linear relationship with the base
604 pair number of *amp^R* segments, suggesting that •OH reacts with all nucleobases of plasmid
605 DNA non-selectively. The rate constants of SO₄•⁻ with *amp^R* segments were an order of
606 magnitude lower than the corresponding •OH rate constants; thus, the contribution of the
607 trace amount of •OH to the overall gene damage cannot be ignored during UV₂₅₄/S₂O₈²⁻
608 treatment.
- 609 • Although •OH and SO₄•⁻ significantly accelerated (~75%) the degradation of *amp^R*
610 amplicons measured by qPCR during UV₂₅₄/H₂O₂ and UV₂₅₄/S₂O₈²⁻ experiments, this only
611 marginally increased the gene deactivation rate (~11%), as gene damage caused by UV₂₅₄
612 and radical co-exposure appeared to be repaired more efficiently by recipient cells than the

613 gene damage from the separate UV₂₅₄ and radical exposures. Thus, the elimination
614 efficiency of the ARGs' transforming activities was similar for UV₂₅₄ vs UV₂₅₄-AOPs at the
615 same UV fluence, and the extent of elimination was mainly determined by the level of UV
616 fluence. Because the transforming activity of the *amp*^R gene could be lowered by only ~1-
617 log at a typical UV disinfection fluence for water treatment (e.g., 40 mJ/cm²) but increased
618 to more than 4-logs at an elevated UV fluence for UV-AOPs (e.g., 500 mJ/cm²), the use of
619 UV-AOPs may still prove beneficial for ARG degradation and deactivation, with the
620 accompanying benefit of improved degradation of trace organic contaminants.

- 621 • Reactive species formed from the excitation of chromophoric organic matter appear to
622 contribute to accelerated degradation of *amp*^R during UV₂₅₄ irradiation in the presence of
623 EfOM (compared to direct photolysis by UV₂₅₄ alone), whereas EfOM mainly acted as a
624 radical scavenger in UV₂₅₄/H₂O₂ and UV₂₅₄/S₂O₈²⁻ experiments.

625 **Acknowledgements**

626 This study was supported by the Korea Institute of Marine Science & Technology Promotion
627 funded by the National Research Foundation funded by the Ministry of Science, ICT and Future
628 Planning (NRF-2020R1A2C2011951). Curtin University (Curtin International Postgraduate
629 Research Scholarship) and Water Research Australia (WaterRA Postgraduate Scholarship) are
630 gratefully acknowledged for providing financial support for M. Nihemaiti. Additional support
631 for H. He and M. C. Dodd from U.S. National Science Foundation Grant Number CBET-
632 1254929 is gratefully acknowledged.

633

634 **Reference**

635 Alberts, B., et al. (2002). Molecular Biology of the Cell, 4th edition. New York, Garland
636 Science.

637
638 Batista, A. P. S., et al. (2016). "Correlating the chemical and spectroscopic characteristics of
639 natural organic matter with the photodegradation of sulfamerazine." Water Research **93**: 20-29.

640
641 Bioneer (2016). "AccuPrep® Nano-Plus Plasmid Mini/Midi/Maxi Extraction Kit." User's Guide
642 **Available at [http://us.bioneer.com/Protocol/AccuPrep%20Nano-](http://us.bioneer.com/Protocol/AccuPrep%20Nano-Plus%20Plasmid%20Extraction%20Kit.pdf)**
643 **Plus%20Plasmid%20Extraction%20Kit.pdf**.

644
645 Bolton, J. R. and K. G. Linden (2003). "Standardization of methods for fluence (UV Dose)
646 determination in bench-scale UV experiments." Journal of Environmental Engineering **129**(3):
647 209-215.

648
649 Buxton, G. V., et al. (1988). "Critical Review of rate constants for reactions of hydrated
650 electrons, hydrogen atoms and hydroxyl radicals ($\cdot\text{OH}/\cdot\text{O}-$) in Aqueous Solution." Journal of
651 Physical and Chemical Reference Data **17**(2): 513-886.

652
653 Cacace, D., et al. (2019). "Antibiotic resistance genes in treated wastewater and in the receiving
654 water bodies: A pan-European survey of urban settings." Water Research **162**: 320-330.

655
656 Cadet, J., et al. (1999). "Hydroxyl radicals and DNA base damage." Mutation
657 Research/Fundamental and Molecular Mechanisms of Mutagenesis **424**(1): 9-21.

658
659 Cadet, J. and T. Douki (2018). "Formation of UV-induced DNA damage contributing to skin
660 cancer development." Photochemical & Photobiological Sciences **17**(12): 1816-1841.

661
662 Chang, P. H., et al. (2017). "Degradation of Extracellular Antibiotic Resistance Genes with
663 UV254 Treatment." Environmental Science & Technology **51**(11): 6185-6192.

664
665 Chin, Y.-P., et al. (2004). "Photosensitized Degradation of Bisphenol A by Dissolved Organic
666 Matter." Environmental Science & Technology **38**(22): 5888-5894.

667
668 Christou, A., et al. (2017). "The potential implications of reclaimed wastewater reuse for
669 irrigation on the agricultural environment: The knowns and unknowns of the fate of antibiotics
670 and antibiotic resistant bacteria and resistance genes – A review." Water Research **123**: 448-467.

671
672 Davies, J. and D. Davies (2010). "Origins and Evolution of Antibiotic Resistance."
673 Microbiology and Molecular Biology Reviews : MMBR **74**(3): 417-433.

674

675 Dizdaroglu, M. and P. Jaruga (2012). "Mechanisms of free radical-induced damage to DNA."
676 Free Radical Research **46**(4): 382-419.

677

678 Dodd, M. C. (2012). "Potential impacts of disinfection processes on elimination and
679 deactivation of antibiotic resistance genes during water and wastewater treatment." Journal of
680 Environmental Monitoring **14**(7): 1754-1771.

681

682 Elovitz, M. S. and U. von Gunten (1999). "Hydroxyl Radical/Ozone Ratios During Ozonation
683 Processes. I. The Rct Concept." Ozone: Science & Engineering **21**(3): 239-260.

684

685 Ferro, G., et al. (2016). "Antibiotic resistance spread potential in urban wastewater effluents
686 disinfected by UV/H₂O₂ process." Science of the Total Environment **560-561**: 29-35.

687

688 Ferro, G., et al. (2017). "β-lactams resistance gene quantification in an antibiotic resistant
689 Escherichia coli water suspension treated by advanced oxidation with UV/H₂O₂." Journal of
690 Hazardous Materials **323**: 426-433.

691

692 Giannakis, S., et al. (2018). "Solar photo-Fenton disinfection of 11 antibiotic-resistant bacteria
693 (ARB) and elimination of representative AR genes. Evidence that antibiotic resistance does not
694 imply resistance to oxidative treatment." Water Research **143**: 334-345.

695

696 Görner, H. (1994). "New trends in photobiology: Photochemistry of DNA and related
697 biomolecules: Quantum yields and consequences of photoionization." Journal of Photochemistry
698 and Photobiology B: Biology **26**(2): 117-139.

699

700 Guo, M.-T., et al. (2015). "Distinguishing Effects of Ultraviolet Exposure and Chlorination on
701 the Horizontal Transfer of Antibiotic Resistance Genes in Municipal Wastewater."
702 Environmental Science & Technology **49**(9): 5771-5778.

703

704 He, H., et al. (2019). "Degradation and Deactivation of Bacterial Antibiotic Resistance Genes
705 during Exposure to Free Chlorine, Monochloramine, Chlorine Dioxide, Ozone, Ultraviolet Light,
706 and Hydroxyl Radical." Environmental Science & Technology **53**(4): 2013-2026.

707

708 Hiller, C. X., et al. (2019). "Antibiotic microbial resistance (AMR) removal efficiencies by
709 conventional and advanced wastewater treatment processes: A review." Science of the Total
710 Environment **685**: 596-608.

711

712 Hong, P.-Y., et al. (2018). "Reusing Treated Wastewater: Consideration of the Safety Aspects
713 Associated with Antibiotic-Resistant Bacteria and Antibiotic Resistance Genes." Water **10**(3).

714

715 Kisker, C., et al. (2013). "Prokaryotic Nucleotide Excision Repair." **5**(3): a012591-a012591.

716

717 Kohn, T., et al. (2007). "Association with Natural Organic Matter Enhances the Sunlight-
718 Mediated Inactivation of MS2 Coliphage by Singlet Oxygen." Environmental Science &
719 Technology **41**(13): 4626-4632.

720
721 Kohn, T. and K. L. Nelson (2007). "Sunlight-Mediated Inactivation of MS2 Coliphage via
722 Exogenous Singlet Oxygen Produced by Sensitizers in Natural Waters." Environmental Science
723 & Technology **41**(1): 192-197.

724
725 Lee, Y., et al. (2016). "Organic Contaminant Abatement in Reclaimed Water by UV/H₂O₂ and
726 a Combined Process Consisting of O₃/H₂O₂ Followed by UV/H₂O₂: Prediction of Abatement
727 Efficiency, Energy Consumption, and Byproduct Formation." Environmental Science &
728 Technology **50**(7): 3809-3819.

729
730 Lester, Y., et al. (2013). "Production of Photo-oxidants by Dissolved Organic Matter During UV
731 Water Treatment." Environmental Science & Technology **47**(20): 11726-11733.

732
733 Liu, S.-S., et al. (2018). "Chlorine disinfection increases both intracellular and extracellular
734 antibiotic resistance genes in a full-scale wastewater treatment plant." Water Research **136**: 131-
735 136.

736
737 Lorenz, M. G. and W. Wackernagel (1994). "Bacterial gene transfer by natural genetic
738 transformation in the environment." Microbiological Reviews **58**(3): 563-602.

739
740 Lorenz, M. G. and W. Wackernagel (1994). "Bacterial gene transfer by natural genetic
741 transformation in the environment." Microbiol. Mol. Biol. Rev. **58**(3): 563-602.

742
743 Luby, E., et al. (2016). "Molecular Methods for Assessment of Antibiotic Resistance in
744 Agricultural Ecosystems: Prospects and Challenges." Journal of Environment Quality **45**(2): 441.

745
746 Lutze, H. V., et al. (2015). "Sulfate radical-based water treatment in presence of chloride:
747 Formation of chlorate, inter-conversion of sulfate radicals into hydroxyl radicals and influence
748 of bicarbonate." Water Research **72**: 349-360.

749
750 Mao, D., et al. (2014). "Persistence of Extracellular DNA in River Sediment Facilitates
751 Antibiotic Resistance Gene Propagation." Environmental Science & Technology **48**(1): 71-78.

752
753 McKinney, C. W. and A. Pruden (2012). "Ultraviolet disinfection of antibiotic resistant bacteria
754 and their antibiotic resistance genes in water and wastewater." Environmental Science and
755 Technology **46**(24): 13393-13400.

756
757 Michael-Kordatou, I., et al. (2015). "Erythromycin oxidation and ERY-resistant Escherichia coli
758 inactivation in urban wastewater by sulfate radical-based oxidation process under UV-C
759 irradiation." Water Research **85**: 346-358.

760
761 Nagler, M., et al. (2018). "Extracellular DNA in natural environments: features, relevance and
762 applications." Applied Microbiology and Biotechnology **102**(15): 6343-6356.

763
764 Nelson, K. L., et al. (2018). "Sunlight-mediated inactivation of health-relevant microorganisms
765 in water: a review of mechanisms and modeling approaches." Environmental Science: Processes
766 & Impacts **20**(8): 1089-1122.

767
768 Neta, P., et al. (1988). "Rate Constants for Reactions of Inorganic Radicals in Aqueous
769 Solution." Journal of Physical and Chemical Reference Data **17**(3): 1027-1284.

770
771 Neta, P., et al. (1977). "Rate constants and mechanism of reaction of SO₄^{·-} with aromatic
772 compounds." Journal of the American Chemical Society **99**(1): 163-164.

773
774 Osińska, A., et al. (2020). "Small-scale wastewater treatment plants as a source of the
775 dissemination of antibiotic resistance genes in the aquatic environment." Journal of Hazardous
776 Materials **381**: 121221.

777
778 Pruden, A. (2014). "Balancing Water Sustainability and Public Health Goals in the Face of
779 Growing Concerns about Antibiotic Resistance." Environmental Science & Technology **48**(1):
780 5-14.

781
782 Rosado-Lausell, S. L., et al. (2013). "Roles of singlet oxygen and triplet excited state of
783 dissolved organic matter formed by different organic matters in bacteriophage MS2
784 inactivation." Water Research **47**(14): 4869-4879.

785
786 Rosario-Ortiz, F. L. and S. Canonica (2016). "Probe Compounds to Assess the Photochemical
787 Activity of Dissolved Organic Matter." Environmental Science & Technology **50**(23): 12532-
788 12547.

789
790 Shanehbandi, D., et al. (2013). "Vibration and glycerol-mediated plasmid DNA transformation
791 for Escherichia coli." FEMS Microbiology Letters **348**(1): 74-78.

792
793 Shinohara, A. and T. Ogawa (1995). "Homologous recombination and the roles of double-strand
794 breaks." Trends in Biochemical Sciences **20**(10): 387-391.

795
796 Shou, W., et al. (2019). "Substituted Aromatic-Facilitated Dissemination of Mobile Antibiotic
797 Resistance Genes via an Antihydrolysis Mechanism Across an Extracellular Polymeric
798 Substance Permeable Barrier." Environmental Science & Technology **53**(2): 604-613.

799
800 Sinha, R. P. and D.-P. Häder (2002). "UV-induced DNA damage and repair: a review."
801 Photochemical & Photobiological Sciences **1**(4): 225-236.

802

803 Smith, K. C. and T.-C. V. Wang (1989). "recA-dependent DNA repair processes." BioEssays
804 **10**(1): 12-16.

805

806 Song, K., et al. (2016). "Application of ultraviolet light-emitting diodes (UV-LEDs) for water
807 disinfection: A review." Water Research **94**: 341-349.

808

809 Stefan, M. I. (2018). Advanced Oxidation Processes for Water Treatment. Fundamentals and
810 Applications, IWA Publishing.

811

812 Teebor, G. W., et al. (1988). "The Repairability of Oxidative Free Radical Mediated Damage to
813 DNA: A Review." International Journal of Radiation Biology **54**(2): 131-150.

814

815 Vikesland, P. J., et al. (2017). "Toward a Comprehensive Strategy to Mitigate Dissemination of
816 Environmental Sources of Antibiotic Resistance." Environmental Science & Technology **51**(22):
817 13061-13069.

818

819 von Sonntag, C. (2006). Free-radical-induced DNA damage and its repair: A chemical
820 perspective. Heidelberg, Berlin, Springer.

821

822 Wu, D., et al. (2019). "Urban and agriculturally influenced water contribute differently to the
823 spread of antibiotic resistance genes in a mega-city river network." Water Research **158**: 11-21.

824

825 Yoon, Y., et al. (2017). "Inactivation efficiency of plasmid-encoded antibiotic resistance genes
826 during water treatment with chlorine, UV, and UV/H₂O₂." Water Research **123**: 783-793.

827

828 Yoon, Y., et al. (2018). "Elimination of transforming activity and gene degradation during UV
829 and UV/H₂O₂ treatment of plasmid-encoded antibiotic resistance genes." Environmental
830 Science: Water Research & Technology.

831

832 Zhang, T., et al. (2019). "Removal of antibiotic resistance genes and control of horizontal
833 transfer risk by UV, chlorination and UV/chlorination treatments of drinking water." Chemical
834 Engineering Journal **358**: 589-597.

835

836 Zhang, X., et al. (2019). "Enhanced Photodegradation of Extracellular Antibiotic Resistance
837 Genes by Dissolved Organic Matter Photosensitization." Environmental Science & Technology
838 **53**(18): 10732-10740.

839

840 Zhang, Y., et al. (2017). "Subinhibitory Concentrations of Disinfectants Promote the Horizontal
841 Transfer of Multidrug Resistance Genes within and across Genera." Environmental Science &
842 Technology **51**(1): 570-580.

843

844 Zhang, Y., et al. (2018). "Cell-free DNA: A Neglected Source for Antibiotic Resistance Genes
845 Spreading from WWTPs." Environmental Science & Technology **52**(1): 248-257.

846
847 Zheng, J., et al. (2017). "Effects and mechanisms of ultraviolet, chlorination, and ozone
848 disinfection on antibiotic resistance genes in secondary effluents of municipal wastewater
849 treatment plants." Chemical Engineering Journal **317**: 309-316.

850
851 Zheng, X., et al. (2014). "Contribution of effluent organic matter (EfOM) to ultrafiltration (UF)
852 membrane fouling: Isolation, characterization, and fouling effect of EfOM fractions." Water
853 Research **65**: 414-424.

854

855

Graphical Abstract

